Leak Width of a Cusp-Confined Plasma

G. Knorr and D. Willis

Department of Physics and Astronomy. The University of Iowa, Iowa City, U.S.A.

Z. Naturforsch. **37a**, 780–785 (1982); received March 12, 1982

To Professor Arnulf Schlüter on his 60th Birthday

The theoretical and numerical steady-state calculation of the width of an escaping plasma stream through a magnetic mirror solves the self-consistent potential and charge distribution for a low beta plasma. The leak width is obtained as the geometric mean of the ion and electron Larmor radius, also called hybrid width, in agreement with some experimental measurements. If the out-streaming plasma is unstable or collisional, the leak width can only larger, contrary to earlier results in the literature.

1. Introduction

If a plasma is confined on one side of a magnetic picket fence (compare Fig. 1), it escapes through the magnetic mirror forming a stream of a certain half-width which is called the leak width. In this paper, we consider how this width scales. This question has been discussed extensively, however, the answers given are not unique. Some authors say the leak width scales with the ion Larmor radius r_i, others claim that it scales with the hybrid width $r_h = \sqrt{r_i r_e}$, where r_i and r_e are the ion and electron Larmor radii, respectively. The Larmor radii are calculated using the magnetic field strength in the center of the mirror, but the temperatures are taken from the bulk of the confined plasma. In a review article, Haines [1] discusses the experiments of Kitsunezaki et al. [2], Hershkowitz et al. [3], and Leung et al. [4], who all found the hybrid leak width. Haines holds out ion-acoustic instabilities and the viscoresistive sheath as possible explanations. In a more recent paper, Hershkowitz et al. [5] find the hybrid width in their investigation of the electrostatic self-plugging of a picket fence. But in a laser-produced plasma in a spindle cusp, Kogoshi et al. [6] find essentially an ion Larmor radius leak width. Only at early times in their experiment is a leak width of the order of a hybrid radius found, and they are then working with the rather high-beta value of 0.6. Pechacek et al. [7] also find a leak width of an ion Larmor radius; they too work with a laser-produced plasma in an spindle cusp. The two-dimensional particle simulation of Marcus et al. [8] indicates that the plasma flow is nonturbulent. The leak width is not inconsistent with a hybrid radius. Unfortunately, no clear-cut conclusion can be drawn from this simulation, as the ratio m_e/m_i had to be chosen unrealistically large to make electron and ion time scales commensurable. In unpublished studies, Lamm [9] finds experimentally, and Samec [10] theoretically, that the width is an ion Larmor radius. Both criticize the work of [3] and [4]. The recent experiments of Cartier [11] also confirm the r_i dependence.

In comparing these experiments, the wide diversity of plasma environments should be borne in

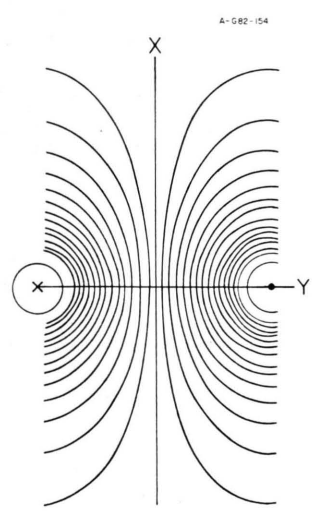

Fig. 1. Magnetic field lines of a picket fence. The centers of circles are the locations of the current-carrying wires. The origin of the coordinate system is the location to which the analytical model approximately applies.

Reprint requests to Dr. G. Knorr, Department of Physics and Astronomy, University of Iowa, Iowa City, Iowa 52242, U.S.A.

0340-4811 / 82 / 0800-0780 $ 01.30/0. — Please order a reprint rather than making your own copy.

mind. Because modes of plasma production and magnetic field geometries vary greatly, the above results may not be so contradictory.

In this paper, we assume a low-beta plasma (as was the case in the experiments of [3] and [4]) and a steady state. We obtain a solution with a self-consistent electric field that gives a half-width of a hybrid radius. Our result puts the argument of Haines [1] in a different light: Any instability or turbulence can only increase the half-width beyond the hybrid value.

2. The Steady-state Model

A theory of the full problem is quite complicated, last but not least because of the complicated field geometry: Far away from the picket fence the magnetic field strength is very small. In fact, it decreases exponentially with the distance from the picket fence, the distance between current-carrying wires being the scale length. In the region close to the picket fence, the field changes fast so that the use of the adiabatic invariance appears dubious. Even if one makes use of the adiabatic invariance, the charge density is a highly nonlinear function of $|B|$ and φ, the electrostatic potential, for which the two-dimensional Poisson equation has to be solved self-consistently, including boundary conditions. The assumption of charge neutrality is unlikely to hold because the plasma inside the mirror forms a sheath, which is intrinsically nonneutral.

In order to understand some of the physics, in particular, the spread of the beam perpendicular to the magnetic field, we adopt a radically simplified model. We assume that the plasma streaming into the mirror can be described at the throat of the mirror as steady-state ion and electron beams with temperatures θ_i and θ_e, respectively, symmetric to the center plane, flowing in a homogeneous magnetic field. If we ignore the electric field, which pulls the ions in and electrons out, the width of each beam is of the order of the species' Larmor radius. Additionally, we assume a particle experiences no collisions in the time it takes to flow into the mirror and either escape from the confinement region or be reflected. Thus a Vlasov-Poisson model is adequate.

We construct stationary solutions of the Vlasov equation using the energy

$$\tfrac{1}{2} m v^2 + q\varphi$$

and the y-component of the generalized momentum,

$$x - v_y/\Omega$$

of a particle as invariants and obtain

$$f(x, v) = A \exp\left[-\frac{\frac{1}{2} m v^2 + q\varphi}{\theta} - \frac{(x - v_y/\Omega)^2}{\alpha^2}\right].$$

Here $m, q, \theta, \Omega = qB/mc$ are the mass, charge, temperature, and gyrofrequency of a particle, α is a so far undetermined constant, of dimension length. Integrating over all velocities, we obtain the particle density

$$n(x) = \int f \, dv_x \, dv_y \, dv_z = \frac{A (2\pi)^{3/2} (\theta/m)^{3/2}}{\sqrt{1 + 2 r_L^2/\alpha^2}} \cdot \exp\left(-\frac{x^2}{2 r_L^2 + \alpha^2} - \frac{q\varphi}{\theta}\right), \quad (1)$$

where we have introduced the Larmor radius $r_L^2 = \theta/(m\Omega^2)$ of the species in question. It is seen that α determines the width of the beam, the larger α, the wider the beam. We choose, somewhat arbitrarily, $\alpha = 2 r_L^2$, which makes the half-width of the beam equal to $2\sqrt{\ln 2} = 1.7$ Larmor radii, if the self-consistent field is ignored. A different factor would merely change numerical coefficients but not the scaling with the physical parameters. We expect such a beam diameter from the converging flow in a magnetic mirror, assuming an approximate constancy of the adiabatic invariant.

We introduce the dimensionless quantities $\xi = x/r_{Le}$ and $\varphi(\xi) = q\varphi/\theta_e$. Thus length and potential are scaled to electron Larmor radius and temperature. The Poisson equation can now be written as

$$\frac{d^2}{d\xi^2}\varphi(\xi) = -C^2[\lambda \exp(-\tfrac{1}{4}\varepsilon^2\xi^2 - R^{-1}\varphi) - \exp(-\tfrac{1}{4}\xi^2 + \varphi)]. \quad (2)$$

There are three dimensionless constants in Eq. (2):

$$R = \theta_i/\theta_e,$$

$$\varepsilon = r_e/r_i = \sqrt{m_e/(m_i R)}, \quad \text{and}$$

$$C = r_e/\lambda_{De} = r_e/\sqrt{\theta_e/(4\pi q^2 n_0 e)}.$$

Note that for $R = 0(1)$, ε is small; e.g., for an equal temperature hydrogen plasma, $\varepsilon = 1/43$. C can be greater than or less than one in experiments. In [3] it was of order one. The ratio $\lambda = n_{0i}/n_{0e}$ of the ion to electron density at the symmetry plane $x = 0$ will be determined by the boundary conditions.

The first term on the right of (2) is the ion density, the second the electron density. By symmetry, the boundary condition at $\xi=0$ is

$$\varphi(0)=\varphi'(0)=0\,. \tag{3}$$

Since we want an equal number of electrons and ions in a cross section, i.e.,

$$\int_0^\infty n_\mathrm{i}\,\mathrm{d}\xi=\int_0^\infty n_\mathrm{e}\,\mathrm{d}\xi\,,$$

we require

$$\varphi'(\infty)=0\,. \tag{4}$$

The problem would be overdetermined if we could not simultaneously satisfy the three boundary conditions by the adjustment of $\lambda=n_{0\mathrm{i}}/n_{0\mathrm{e}}$. Equation (2), together with boundary conditions (3) and (4), is a highly nonlinear boundary-value/eigenvalue problem. An analytical solution appears to be out of the question.

3. The Model

We can, however, write (2) as

$$\varphi''=-\,C^2[\lambda g(\varepsilon\xi)\exp(-\,R^{-1}\varphi)-g(\xi)\exp(\varphi)]\,, \tag{5}$$

with $g(\xi)=\exp(-\tfrac{1}{4}\xi^2)$. Rather than choosing the function $g(\xi)$ as in (2), we select a $g(\xi)$ for analytical convenience. If g is the step function

$$g(\xi)=\begin{cases}1, & 0\leqq\xi\leqq\xi_0=2\alpha;\\ 0, & \xi>\xi_0\,,\end{cases} \tag{6}$$

Eq. (5) splits up into two equations that do not involve the independent variable and so become analytically tractable. Comparison with accurate numerical solutions of (2) shows that our model (6) gives solutions close to the exact solutions of (2). It is, however, much simpler to deal with asymptotic limits analytically. We obtain

$$\varphi''=-\,C^2[\lambda\exp(-\,R^{-1}\varphi)-\exp(\varphi)]\,,\quad 0\leqq\xi\leqq\xi_0; \tag{7}$$

$$\varphi''=-\,C^2\lambda\exp(-\,R^{-1}\tilde{\varphi})\,,\quad \xi_0\leqq\xi\leqq\xi_\mathrm{m}=\xi_0/\varepsilon\,. \tag{8}$$

The boundary condition (4) is replaced by $\varphi'(\xi_0/\varepsilon)=0$, also φ and φ' must be continuous at $\xi=\xi_0$:

$$\varphi(\xi_0{}^+)=\varphi(\xi_0{}^-);\quad \varphi'(\xi_0{}^+)=\varphi'(\xi_0{}^-)\,. \tag{9}$$

α must be of order one so that the step function (6) can optimally approximate the exponentials in (2).

Equations (7) and (8) can be integrated explicitly, if we only assume that $\varphi(\xi_0)\ll 1$, so that (7) can be linearized. We find

$$\varphi(\xi)=\tfrac{1}{2}C^2(1-\lambda)\xi^2\,,\quad 0\leqq\xi\leqq\xi_0=2\alpha; \tag{10}$$

$$\varphi(\xi)=\varphi_\mathrm{m}+R\ln[\cos^2W(\xi_\mathrm{m}-\xi)]\,,\quad \xi_0\leqq\xi\leqq\xi_\mathrm{m}=2\alpha/\varepsilon\,, \tag{11}$$

where

$$W=[\lambda C^2/2R\exp(-\,R^{-1}\varphi_\mathrm{m})]^{1/2}\,. \tag{12}$$

Solving (12) for φ_m gives

$$\varphi_\mathrm{m}=R\ln\frac{\lambda C^2}{2RW^2}\,, \tag{13}$$

which, when inserted into (11), yields

$$\varphi(\xi)=R\ln\left[\frac{\lambda C^2}{2RW^2}\cos^2W(\xi_\mathrm{m}-\xi)\right].$$

Continuity of $\varphi(\xi)$ and $\varphi'(\xi)$ at $\xi=\xi_0$ gives two conditions which determine λ and W (or φ_m).

$$\varphi(\xi_0)=\varphi_0=R\ln\cdot\left[\frac{\lambda C^2}{2RW^2}\cos^2W(\xi_\mathrm{m}-\xi_0)\right], \tag{14}$$

$$\varphi'(\xi_0)=\varphi_0{}'=2RW\tan W(\xi_\mathrm{m}-\xi_0)\,, \tag{15}$$

where

$$\varphi_0=2(1-\lambda)\,C^2\alpha^2\,, \tag{16}$$

and

$$\varphi_0{}'=2(1-\lambda)\,C^2\alpha\,. \tag{17}$$

We evaluate now the asymptotic behavior of λ and φ_m as $\varepsilon\to 0$. Clearly, $\xi_\mathrm{m}=2\alpha/\varepsilon\to\infty$. If W would tend to a constant value different from zero for $\varepsilon\to 0$, $\varphi_0{}'$ would by (15) go periodically to infinity. This is unphysical and we conclude that $\lim_{\varepsilon\to 0}W=0$. The value $\lambda=1$ will be assumed for $\varepsilon=1$ and $R=1$ for symmetry reasons because then electrons and ions have equal mass and the same Larmor radius. If $\varepsilon<1$, the electron Larmor radius will be smaller, electrons will be more concentrated in the center, i.e., $\lambda<1$. Then, by (16) and (17), φ_0 and $\varphi_0{}'$ will have values greater than zero. It follows that, because of (15),

$$\lim_{\varepsilon\to 0}W(\xi_\mathrm{m}-\xi_0)=\pi/2\,. \tag{18}$$

We write $W(\xi_m - \xi_0) = \pi/2 - \delta$, for small but finite ε.

Equation (15) gives us for lowest order in ε

$$\delta = \frac{\pi}{2} \frac{\varepsilon R}{\alpha \varphi_0'} . \tag{19}$$

With these results it is possible to evaluate Eq. (14) asymptotically to give

$$\varphi_0 = R \ln \frac{2 \lambda C^2 R}{\alpha^2 \varphi_0'^2} . \tag{20}$$

Making use of (16) and (17) we obtain from (20) a transcendental equation for λ as a function of R, C and α.

$$\ln \frac{2 C^2 \alpha^2}{R} + \frac{2 C^2 \alpha^2}{R} (1 - \lambda) = \ln \frac{\lambda}{(1-\lambda)^2} . \tag{21}$$

Figure 2 shows λ as a function of

$$a = 2 C^2 \alpha^2 / R = 2 \alpha^2 (\lambda_{\mathrm{re}}^2 / \lambda_{\mathrm{De}}^2)(\theta_e/\theta_i) .$$

For large $\lambda_{\mathrm{re}}/\lambda_{\mathrm{De}}$ the deviation form charge neutrality in the center plane is small, however, if $r_e = \lambda_{\mathrm{De}}$ and $\theta_i = \theta_e$, the charge neutrality is appreciably violated, $\lambda \sim 0.6$ or $(n_e - n_i)/n_e \approx 40\%$. We insert relation (18) into (12) and obtain for the maximum potential

$$\varphi_m = R \ln \frac{8 \alpha^2 C^2 \lambda}{\pi^2 R \varepsilon^2} . \tag{22}$$

The depth of the potential trough increases logarithmically with the ion mass ($\varepsilon = \sqrt{1/R \cdot m_e/m_i}$) and

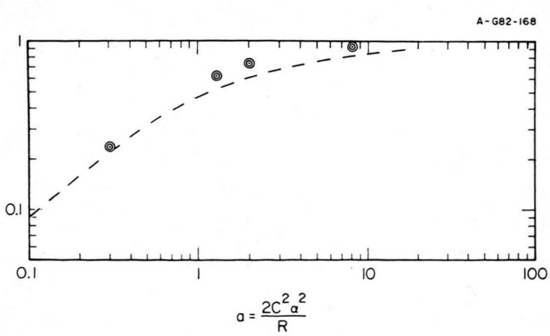

Fig. 2. $\lambda = n_{0i}/n_{0e}$, the ratio of ion to electron density as a function of $a = 2C^2\alpha^2/R = 2\alpha^2(r_e^2/\lambda_{\mathrm{De}}^2)(\theta_e/\theta_i)$. If $r_e/\lambda_{\mathrm{De}}$ is large, the deviation from neutrality is small, for $r_e = \lambda_{\mathrm{De}}$ and $\theta_e = \theta_i$, $(a \approx 2)$, $\lambda \sim 0.6$, i.e., the charge seperation is $\sim 40\%$. The double circled points refer to numerical integration of (2).

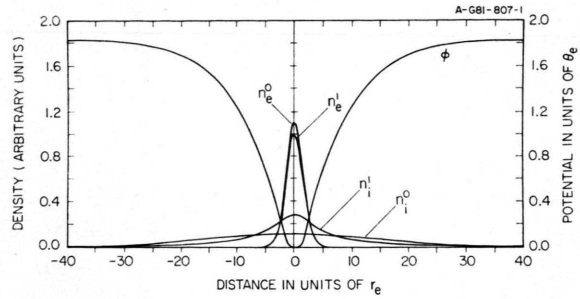

Fig. 3. Illustration of the one-dimensional slab geometry. Curves n_i^0 and n_e^0 are the ion and electron densities if the electric field is switched off. With self-consistent potential $\varphi(\xi)$, the ion density n_i^1 is pulled in, the electron density n_e^1 is — hardly noticeably — pushed out. The curves are a numerical solution of (2) for $C = 0.2$, $\epsilon = 0.8$, $\lambda \approx 0.81$.

has the qualitative shape shown in Figure 3. For example, for $\alpha = 1$, $C = 1$, $\lambda = 0.6$, $R = 1$, and $\varepsilon = 1/43$, we find $q\varphi_m \sim 6.8\,\theta_e$. As R is usually less than one, we expect the potential to be a few times the electron temperature. For later reference we note that the value of W, which follows from (22) and (12), is

$$W = \pi \varepsilon / 4 \alpha . \tag{23}$$

The experiments published in the literature have concentrated on determining the half-width of the potential trough. We obtain the half-width ξ_H by putting $\varphi(\xi) = \frac{1}{2}\varphi_m$ in (11), assuming $\xi_H \geqq \xi_0$. Making use of the expression (22) for φ_m results in

$$\ln \left(\frac{8 \alpha^2 C^2 \lambda}{\pi^2 R \varepsilon^2} \right)^{-1/4} = \ln \cos W (\xi_m - \xi_H) . \tag{24}$$

Exponentiating (24), inserting $\xi_m = 2\alpha/\varepsilon$ and (23) for W gives

$$\sin \frac{\pi}{4} \frac{\varepsilon}{\alpha} \xi_H = \left(\frac{8 \alpha^2 C^2 \lambda}{\pi^2 R \varepsilon^2} \right)^{-1/4} .$$

For small ε the argument on the left side becomes small and the sine can be replaced by its argument. The result is

$$\xi_H = A \, \varepsilon^{-1/2} \tag{25}$$

with

$$A = \left(\frac{32 R \alpha^2}{\pi^2 C^2 \lambda} \right)^{1/4} .$$

Writing this formula in dimensional form gives the physical half-width

$$x_H = A \sqrt{r_i r_e} . \tag{26}$$

In other words, the half-width scales with the hybrid radius or with $m_i^{1/4}$. A is mostly of order one, the experimental values is ~ 2 so that functionally and numerically our result agrees with the experimental measurements of [3—5]. For example, for $R=1$, $\alpha=1$, $C=1$, $\lambda=0.6$, we obtain $A=1.52$. The potential is almost exclusively produced by the ions, the electron density dropping to zero from $\xi_0=2\alpha$ on, which is less than the half-width ξ_H.

The constant α was so far treated as a constant of order one. If we choose α such that the cutoff of $g(x)$ in (6) coincides with the half-width of

$$\exp(-\tfrac{1}{4}x^2),$$

we obtain $\alpha=0.83$. If we equate the areas under $\exp(-\frac{1}{4}x^2)$and $g(x)$ in $0 \leqq x \leqq \infty$, we obtain

$$\alpha=\sqrt{\pi}/2=0.88.$$

Another argument that $\alpha=0(1)$ is the following. The double circled points in Fig. 2 are values of λ obtained from numerical integrations of (2) for small ε and plotted in the figure with $\alpha=1$. They all lie close to and above the curve obtained by the model. As λ increases with ε and the ε used for the computations are small but not zero, this indicates that the model is qualitatively a good approximation to the solution of (2). For convenience we choose $\alpha=1$.

4. The Numerical Solution

The analytical model gives only an approximate solution of (2). We would like to know how accurately the model describes the true solution of (2). Even though this is only an ordinary differential equation, the numerical solution is complicated by the following features.

(1) It is a boundary-value problem.

(2) The differential equation is highly nonlinear.

(3) It is an eigenvalue problem insofar as λ has to be determined such that the boundary conditions $\varphi(0)=\varphi'(0)=\varphi'(\infty)=0$ are all satisfied.

(4) Because we are interested in small ε, there are two distinct length scales, namely $0(1)$ and $0(1/\varepsilon)$.

We will not go into the details of the computations here, they will be discussed elsewhere [14]. Suffice it to say, we have done shooting methods and boundary-value methods. A typical solution curve is shown in Figure 3. Of particular interest is the numerical determination of the half-width of the potential trough as a function of ε. This is shown in Fig. 4 for various parameters C. The curve labeled EX represents the experimental results by Hershkowtiz et al., the cirves labeled M refer to solutions of the model discussed in the previous paragraph, and label N refers to numerical solutions. It is evident that as $\varepsilon \to 0$, the slope of all curves tends to $(-\frac{1}{2})$. Also, all curves are, up to a factor of 4, in agreement with the experimental curve. More numerical data for $\varepsilon < 1/50$ and $C \geqq 1$ would have been desirable. However, it turned out that in this parameter region, the iterations of the code converged very slowly so that only few data could be taken.

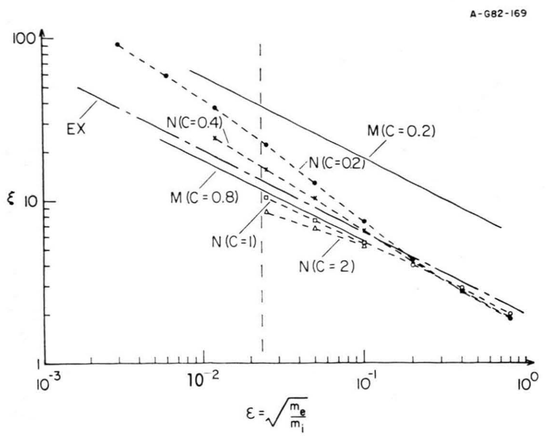

Fig. 4. The half-width ξ_H of the electrostatic potential as a function of $\epsilon=\sqrt{m_e/m_i}$. The designation of the labels are: EX = experimental measurements by Hershkowitz et al., M = analytical model, and N = numerical integration of (2). The values of $C=r_e/\lambda_{De}$ (electron Larmor radius over Debye length) are given in parenthesis. As $\epsilon \to 0$, all curves have the slope $(-\frac{1}{2})$, indicating that the half-width of the potential $\varphi(\xi)$ scales with $m_i^{1/4}$] (compare Figure 3).

5. Conclusions

We have shown that a steady-state, collisionless, low-beta solution with self-consistent electric fields gives a leak width of the order of a hybrid radius. As already mentioned, if there are instabilities and/or turbulence, or if collisions can no longer be neglected, the leak width can only be larger. The question that remains is: Have the experimenters who found a hybrid width succeeded, where the others have not, in eliminating instabilities and collisions?

Recent experiments indicate that fast primary electrons appear to be essential for the existence of potential structures which lead to leaks of the order of a hybrid width. If the primary electrons are excluded from the cusp region, for example by grids, the potential structures become less pronounced and the leak width widens [12—13]. The mechanism of this effect is not understood.

The cusp geometry is one of the simplest MHD-stable configurations. It appears that this question deserves further experimental investigation. A definite answer would not only enhance our basic understanding of plasmas, but could also have important practical consequences.

Acknowledgements

Numerous discussions with Drs. N. Hershkowitz and R. T. Carpenter are gratefully acknowledged. This work was supported in part by U.S. Department of Energy grant DE-ACO2-76ET53034.

[1] M. G. Haines, Nucl. Fusion **17**, 811 (1977).
[2] A. Kitsunezaki, A. Tanimoto, and T. Sekiguchi, Phys. Fluids **17**, 1895 (1974).
[3] N. Hershkowitz, K. N. Leung, and T. Romesser, Phys. Rev. Lett. **35**, 277 (1975).
[4] K. N. Leung, N. Hershkowitz, and K. R. MacKenzie, Phys, Fluids **19**, 1046 (1976).
[5] N. Hershkowitz, J. R. Smith, and H. Kozima, Phys. Fluids **22**, 122 (1979).
[6] S. Kogoshi, K. N. Sato, and T. Sekiguchi, J. Phys. D **11**, 1057 (1978).
[7] R. E. Pechacek, J. R. Greig, M. Raleigh, D. W. Koopman, and A. W. DeSilva, Phys. Rev. Lett. **45**, 256 (1980).
[8] A. J. Marcus, G. Knorr, and G. Joyce, Plasma Phys. **22**, 1015 (1980).
[9] A. J. Lamm, Ph. D. thesis, Department of Physics, University of California, Los Angeles 1976.
[10] T. K. Samec, Ph. D. thesis, Department of Physiks, University of California, Los Angeles 1976.
[11] S. Cartier, Master's thesis, Department of Physics and Astronomy, The University of Iowa, Iowa City 1980.
[12] K. N. Leung, private communication.
[13] R. T. Carpenter, private communication.
[14] D. Willis and G. Knorr, A Nonlinear Eigenvalue/boundary-value Problem, submitted for publication in J. Comput. Physics.